

# Estimating focus and radial distances, and fault residuals from CD player sensor signals by use of a Kalman estimator

P.F. Odgaard, J. Stoustrup, P. Andersen H.F. Mikkelsen

Department of Control Engineering  
Aalborg University  
DK 9220 Aalborg  
{odgaard,jakob,pa}@control.auc.dk

B&O Audiovisual a/s  
Peter Bangs vej 15  
DK 7600 Struer  
hfm@bang-olufsen.dk

## Abstract

Optical cross coupling between focus and radial loops in Compact Disc players is a problem both in nominal operations, but also in detection of defects such as scratches and finger prints. Using a Kalman estimator with an internal reference, the actual focus and radial distances are estimated. The sensor inputs to the Kalman estimator are computed focus and radial distances and are found by solving the inverse problem of an optical model of the Compact Disc player. Two pairs of decoupled fault features are found based on the optical model, estimated and calculated focus and radial errors.

## 1 Introduction

Compact Disc players (CD players) are widely used today, and have been on the market in more than two decades. But there are still performance issues to be improved. It is common to have problems with CDs with surface defects like scratches, finger prints etc. sometimes the CD player jumps to a random track and sometimes it stops playing the disc, as a consequence of the scratch. The problem with these surface defects is that they degenerate the sensor signals used for focusing and radial tracking of the Optical-Pick Unit (OPU). The OPU generates four detector signals, where two of them are used for focus control and the last two are used for radial control. The difference between the two focus signals is, for small focus distances, proportional to the focus distance. The radial detector signal distance is also proportional to the radial difference. This means that the two differences are used as approximations of focus and radial distances. Unfortunately a surface defect would change these differences even though that the real distance does not change. This is one of the reasons why CD players have problems playing discs with surface defects. A common used way to handle these defects is to use either the sum of focus signals or the sum of the radial signals to detect the occurrence of the defect, since a defect would typically lower these sums, see (Philips, 1994), (Andersen *et al.*, 2001) and (Vidal *et al.*, 2001b). One used method to handle such defects is to not rely on sensor information while passing the defect. In some systems the

sensor signals are fixed to zero while passing the defect.

It would be very interesting if it would be possible to estimate focus and radial distance better based on the four detector signals, partly because this would make it possible to extract fault parameters which are not dependent on the actual focus and radial distance, but also as inputs to nominal focus and radial controllers, since these estimated distances are decoupled from each other, in contrast to the normal used difference of the detector signal pairs. In (Odgaard *et al.*, 2003a) a method is proposed which calculates focus and radial distances by solving the inverse problem of the mapping  $(D_1, D_2, S_1, S_2) = f_e(e_f(n), e_r(n), \alpha_f(n), \alpha_r(n))$ . ( $n$ ) means at the discrete time  $n$ .  $D_1, D_2, S_1, S_2$  are the four detector signals and  $e_f(n), e_r(n)$  are focus and radial distances, in this solution a model of defects are incorporated as well. The computed distances are the output of this algorithm,  $\hat{e}_f(n)$  and  $\hat{e}_r(n)$ . This means that the algorithm can still solve the inverse problem even though a defect occurs. The mapping  $f(e_f(n), e_r(n))$  is a model of the optical detector system in the OPU, and such a model is developed in (Odgaard *et al.*, 2003b), for a CD player with a 3 beam single Foucault detector system, as used in the experimental work. Due to measuring noise and fault model errors these calculated focus and radial distances  $\hat{e}_f(n)$  and  $\hat{e}_r(n)$  deviate from the actual values. This can be viewed upon as measurement noise.

In this paper a Kalman observer is designed for estimating focus and radial distances  $(\hat{e}_f, \hat{e}_r)$ . These estimated distances can then be used as inputs to a controller, controlling the OPU in focus and radial direction.  $(\hat{e}_f, \hat{e}_r)$  can also be used to estimate the four detector signals, by computing:  $(\hat{D}_1, \hat{D}_2, \hat{S}_1, \hat{S}_2) = f(\hat{e}_f, \hat{e}_r)$ . These estimated detector signals can be seen as a part of the detector signal which is due to the actual focus and radial distance. The difference between the estimated and measured detector signals is an approximation of the defect in the four detector signals. In this paper some fault parameters, which are based on different fault models, are extracted from these four deviations, and from  $\hat{e}_f$  and  $\hat{e}_r$ . This strategy is illustrated in Fig. 1.

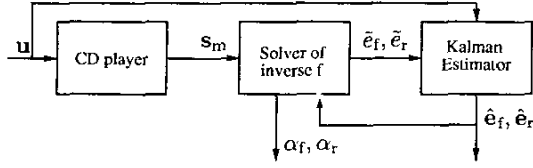


**Figure 1:** The structure of the method described in this paper. The method consists of two parts, which estimates fault parameters,  $(\alpha_f, \alpha_r)$ , focus distance and radial distance from the detector signals. The parts of the method are: inverse problem solver and Kalman estimator.  $u$  is the control signals to the CD player,  $s_m$  is the measured detector signals,  $\tilde{e}_f, \tilde{e}_r$  is the static estimated focus and radial distances, and  $\hat{e}_f, \hat{e}_r$  is the dynamical estimated focus and radial distances.

## 2 Model of the OPU

The OPU is a 2-axis device, enabling a movement of OPU vertically for focus correction and horizontally for radial correction. Linear electro-magnetic actuators are used for both focus and the radial corrections. The magnetic field in the actuators is controlled by focus and radial control voltages  $u_f$  and  $u_r$ . The OPU itself can be modelled as a mass-spring-damper system, with one or two masses dependent on the needed details. This ends in a second or fourth order model for both focus and radial, see (Stan, 1998), (Vidal *et al.*, 2001a) and (Bouwhuis *et al.*, 1985). In (Vidal *et al.*, 2001a) a system identification on the same CD player setup, as used for experimental work in this paper, is performed. The second order model found in (Vidal *et al.*, 2001a) will be used in this paper. Focus and radial models are of the following structure:

$$\dot{\eta}(t) = \begin{bmatrix} -a_0 & -a_1 \\ 1 & 0 \end{bmatrix} \cdot \eta(t) + \begin{bmatrix} 1 \\ 0 \end{bmatrix} \cdot u(t), \quad (1)$$

$$e(t) = \begin{bmatrix} 0 & b \end{bmatrix} \cdot \eta(t). \quad (2)$$

Where  $a_0, a_1, b$  are model parameters. The values  $a_0, a_1, b$  of are found in (Vidal *et al.*, 2001b).

### 2.1 Internal reference model

The reference signals to focus and radial loops are unknown, the nature of these references is eccentricity, skewness of disc etc. Handling these unknown reference need an expansion of the models, used for the Kalman observer, with an internal reference model. It is known that the first and most dominant harmonic of the unknown reference is the angular velocity of the disc. The interval of the angular velocity can be retrieved from (Stan, 1998) to be 4 – 9 Hz. The reference is modelled by a bandpass filter with bandpass region from 4 to 9 Hz. The model will be of the structure:

$$\dot{\eta}_{ref}(t) = \mathbf{A}_{ref} \cdot \eta_{ref}(t) + \mathbf{E} \cdot d_{ref}(t), \quad (3)$$

$$e_{ref} = \mathbf{C}_{ref} \cdot \eta_{ref}(t). \quad (4)$$

Now it is possible to merge the internal reference model together with focus and radial models, and the new extended

models can thereby be achieved.

$$\dot{\eta}(t) = \mathbf{A}_{CD} \cdot \eta(t) + \mathbf{B}_{CD} \cdot u(t) + \mathbf{E} \cdot d_{ref}(t), \quad (5)$$

$$\begin{bmatrix} e_f(t) \\ e_r(t) \end{bmatrix} = \mathbf{C}_{CD} \cdot \eta(t). \quad (6)$$

Where

$$\mathbf{A}_{CD} = \begin{bmatrix} \mathbf{A}_f & 0 & 0 & 0 \\ 0 & \mathbf{A}_{ref} & 0 & 0 \\ 0 & 0 & \mathbf{A}_r & 0 \\ 0 & 0 & 0 & \mathbf{A}_{ref} \end{bmatrix}, \quad (7)$$

$$\mathbf{B}_{CD} = \begin{bmatrix} \mathbf{B}_f & 0 \\ 0 & 0 \\ 0 & \mathbf{B}_r \\ 0 & 0 \end{bmatrix}, \quad (8)$$

$$\mathbf{C}_{CD} = \begin{bmatrix} \mathbf{C}_f & \mathbf{C}_{ref} & 0 & 0 \\ 0 & 0 & \mathbf{C}_r & \mathbf{C}_{ref} \end{bmatrix}. \quad (9)$$

Where  $\mathbf{A}_f, \mathbf{B}_f, \mathbf{C}_f$  are the model matrices in the focus model, and  $\mathbf{A}_r, \mathbf{B}_r, \mathbf{C}_r$  are the model matrices in the radial model. The angular velocity is the same for both, meaning both references have the same frequency content. However, their the absolute values are not necessarily the same. As a consequence an internal reference model is used for both focus and radial loop.

The idea is to use the Kalman estimator in a CD player, meaning that it would be implemented in discrete time. I.e. a discrete time Kalman estimator has to be designed based on a discretized model. The discretization is done by using a zero order hold method with the system's sample frequency at 35kHz.

## 3 Kalman estimator

Before designing a Kalman estimator the discrete time model is expanded to include state and measurement noises as well. The model is then:

$$\eta[n+1] = \Phi \cdot \eta(n) + \Gamma \cdot u(n) + \Psi \cdot \begin{bmatrix} w_1(n) \\ w_2(n) \end{bmatrix}, \quad (10)$$

$$\begin{bmatrix} e_f(n) \\ e_r(n) \end{bmatrix} = \mathbf{C}_{CD} \cdot \eta(n) + \begin{bmatrix} v_1(n) \\ v_2(n) \end{bmatrix}. \quad (11)$$

Where:  $\Phi, \Gamma$  are the discrete time version of  $\mathbf{A}_{CD}, \mathbf{B}_{CD}$ .  $w_1(n), w_2(n), v_1(n), v_2(n)$  are stochastic noises. In the design it is assumed that the  $w_1(n), w_2(n)$  can be viewed as noises added to the control signal. The variance of  $\mathbf{w}$  is named  $\mathbf{Q}$ , the variance of  $\mathbf{v}$  is named  $\mathbf{R}$ , and the covariance is zero. These variance values are unknown and are as consequence used as tuning parameters in the design process of the Kalman estimator. Due to the fact that the CD player will run for a very long time, it is chosen to design a steady state Kalman estimator, see (Franklin *et al.*, 1998). This means that, the steady state Kalman gain,  $\mathbf{L}_{\infty}$ , and steady state innovation gain,  $\mathbf{M}_{\infty}$ , are to be found. The

estimator equations are:

$$\hat{\eta}[n+1] = (\Phi - \mathbf{L}_\infty \cdot \mathbf{C}_{CD}) \cdot \hat{\eta}(n) + \Gamma \cdot \mathbf{u}(n) \quad (12)$$

$$+ \mathbf{L}_\infty \cdot \begin{bmatrix} \tilde{e}_f(n) \\ \tilde{e}_r(n) \end{bmatrix}, \quad (13)$$

$$\begin{bmatrix} \hat{e}_f(n) \\ \hat{e}_r(n) \end{bmatrix} = \mathbf{C}_{CD} \cdot (\mathbf{I} - \mathbf{M}_\infty \cdot \mathbf{C}_{CD}) \cdot \hat{\eta}(n) \quad (14)$$

$$+ \mathbf{C}_{CD} \cdot \mathbf{M}_\infty \cdot \begin{bmatrix} \tilde{e}_f(n) \\ \tilde{e}_r(n) \end{bmatrix}. \quad (15)$$

The two gains are calculated by use of the Matlab function *kalman*, this function has the variance matrices as inputs, and they are found during an iterative design process of the Kalman estimator. The output of this Kalman estimator is illustrated for two experimental examples in Figs. 3 and 7. From these examples it can be seen that the Kalman estimator is well tuned.

#### 4 Fault models

The four detector signals give redundant information for restoring  $e_f$  and  $e_r$ . In (Odgaard *et al.*, 2003a) the following definition is given

**1 DEFINITION (THE DISTURBANCE SET)** *The disturbance set  $\mathcal{D} \in \mathbb{R}^4$  is defined as the set in which any sample  $\mathbf{s}_m$  in  $\mathbb{R}^4$  of the detector signals, will be if only disturbances occurs.*

This means that if only disturbances occur,  $\mathbf{s}_m(n) \in \mathcal{D}$ , but if faults also occur,  $\mathbf{s}_m(n)$  is not inside  $\mathcal{D}$ .  $\mathbf{s}(n)$  may be split into a part which is in  $\mathcal{D}$  caused by  $e_f(n)$  and  $e_r(n)$ , and a part caused by a fault. Two parameters,  $e_f, e_r$ , parametrise the part inside  $\mathcal{D}$ , leaving two parameters for parametrising the fault. In the following some candidates for pairs of two parameters are described.

The two focus detectors are defined as  $D_1(n), D_2(n)$  and the two radial detectors is defined as  $S_1(n), S_2(n)$ , the estimated detector signals are defined as follows:  $\hat{\mathbf{s}}(n) = (\hat{D}_1(n), \hat{D}_2(n), \hat{S}_1(n), \hat{S}_2(n)) = \mathbf{f}(\hat{e}_f(n), \hat{e}_r(n))$ , no fault signals. It is now possible to define two residuals which are good candidates as fault parameters:

$$r_f(n) = \left\| \begin{bmatrix} D_1(n) - \hat{D}_1(n) \\ D_2(n) - \hat{D}_2(n) \end{bmatrix} \right\|, \quad (16)$$

$$r_r(n) = \left\| \begin{bmatrix} S_1(n) - \hat{S}_1(n) \\ S_2(n) - \hat{S}_2(n) \end{bmatrix} \right\|. \quad (17)$$

They can be viewed as the geometric length of the fault in respective focus and radial detector signals. The deviation from  $\mathcal{D}$  for a given sample can be separated into a part relating to the focus signals and a part relating to the radial signals. These two parameters are the length of these separated parts. In addition the parameters are residuals since they are equal zero in case of no faults and increases as the fault develops. This strategy is related to the method

used in industry, see Section 1. However, using (16) the two loops are decoupled.

The next set of fault parameters are based on  $\tilde{e}_f(n)$  and  $\tilde{e}_r(n)$ , since it give a more clear fault parameter using the next fault parameter definition, compared with fault parameters based on the estimated distances. The defect decreases the reflection rate the disc surface, this in basic idea of another fault model in (Odgaard *et al.*, 2003a), where two other fault parameters were described. They are based on the following fault model:

$$\begin{bmatrix} D_1(n) \\ D_2(n) \\ S_1(n) \\ S_2(n) \end{bmatrix} \approx \beta(n) \cdot \begin{bmatrix} \tilde{D}_1(n) \\ \tilde{D}_2(n) \\ \tilde{S}_1(n) \\ \tilde{S}_2(n) \end{bmatrix}. \quad (18)$$

The fault in this model is modelled as variable multiplied with the detector signals. This model is based on experimental results, see (Vidal *et al.*, 2001c). Using this fault model  $\beta(n)$  is an obvious parameter. It is a measure of the fault in a given sample. This model only uses one parameter, and can therefore not guarantee that the fault model can describe the deviation from  $\mathcal{D}$ . Therefore the second parameter is chosen to be a measure of model remain. This measure could be the norm of the difference between the model and measurement:

$$\gamma(n) = \left\| \begin{bmatrix} D_1(n) \\ D_2(n) \\ S_1(n) \\ S_2(n) \end{bmatrix} - \beta(n) \cdot \begin{bmatrix} \tilde{D}_1(n) \\ \tilde{D}_2(n) \\ \tilde{S}_1(n) \\ \tilde{S}_2(n) \end{bmatrix} \right\|, \quad (19)$$

$\gamma(n)$  measures the validity of the model of the fault. If the model is perfect  $\gamma = 0$  and as  $\gamma(n) \rightarrow \infty$  the model's quality decreases.  $\beta(n)$  is not a residual since it is equal one in cases of no faults and decreases in case of a fault. Instead a related residual,  $\alpha(n)$ , can be defined as:

$$\alpha(n) = 1 - \frac{1}{\beta(n)} \quad (20)$$

Two pairs of interesting fault parameters,  $(r_f, r_r)$  and  $(\alpha, \gamma)$ , are now defined. In the following Section, 5, the two pairs are calculated for some interesting signals sampled at the experimental setup.

#### 5 Experimental data

The experimental setup consists of a CD player, with three beam single Foucault detector principle, a PC with an I/O-card, and some hardware in order to connect the CD player with the I/O-card. Due to the limited computational power of the CPU in the PC the sample frequency is chosen to 35 kHz. The four detector signals and the two control signals are sampled. By using the build in controller of the CD player, a number of CDs with certain defects are sampled in a normal operation. Normal operation means that the defects are not severe enough to force the CD player in a state where it cannot play disc, but on the other hand the defect is challenging for the controllers.

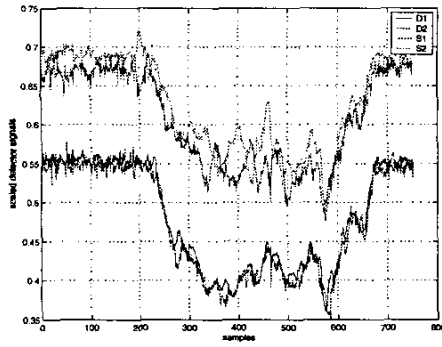


**Figure 2:** Measured detector signals  $D_1(n)$ ,  $D_2(n)$ ,  $S_1(n)$  and  $S_2(n)$  while passing the scratch.

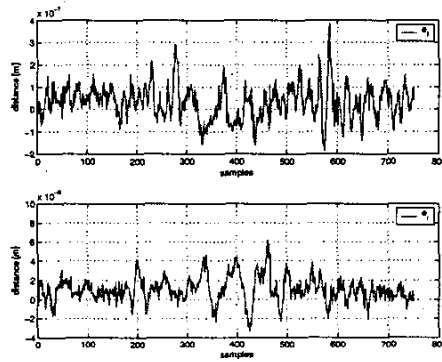


**Figure 3:** Estimated distances  $\hat{e}_f(n)$  and  $\hat{e}_r(n)$  while passing the scratch.

The experimental work has mainly been focused on real scratches and finger prints, since artificial defects tend to be nice and regular, and they are not really challenging. The method has been used on number of different defects, and they all show similar results to the two chosen in this paper. The method is applied to two different faults: a scratch and a finger print. For both the scratch, (S), and the finger print, (F), four plots are shown, illustrating the sampled signals, for (S) see Fig. 2 and for (F) see Figs. 6. The estimated distances ( $\hat{e}_f(n)$ ,  $\hat{e}_r(n)$ ) can for (S) be see in Fig. 3 and can for (F) be see in Figs. 7. The first pair of fault parameters ( $r_f(n)$ ,  $r_r(n)$ ) can for (S) be seen in Fig. 4 and can for (F) be seen in Fig. 8. The second pair of fault parameters  $\alpha(n)$  and  $\gamma(n)$  can for (S) be see in Fig. 5 and can for (F) be seen in Fig. 9.

In the following Figs 2-9 will be commented. Starting with the Figs. 2-5, related to the scratch. Fig. 2 illustrating the scaled detector signals, since it is easy from this figure to do a visual detection of the defect. The defect is the part of the signals where the values are significant lower, it lasts approximately from sample 230 to sample 670. Fig. 3 shows  $\hat{e}_f(n)$  and  $\hat{e}_r(n)$ . By comparing these with  $\bar{e}_f(n)$ ,  $\bar{e}_r(n)$ ,  $u_f(n)$  and  $u_r(n)$ , it can be seen that  $\hat{e}_f(n)$  and  $\hat{e}_r(n)$

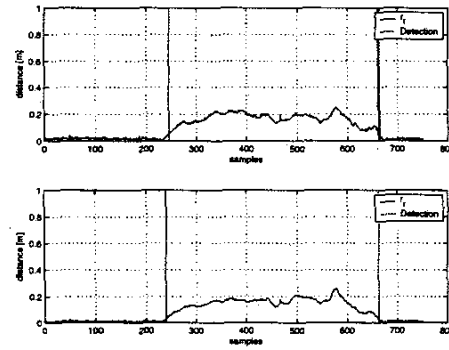


**Figure 4:** The two fault parameters  $r_f(n)$  and  $r_r(n)$  together with their respective threshold detection while passing the scratch.

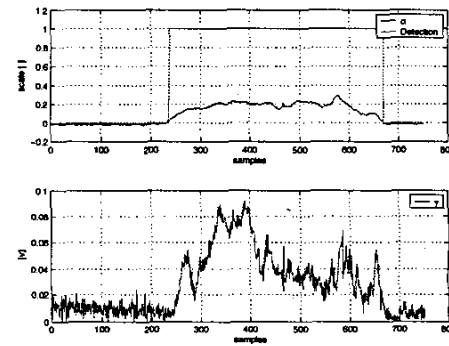


**Figure 5:** The fault parameters  $\alpha(n)$  and  $\gamma(n)$ , and threshold based fault detection while passing the scratch.

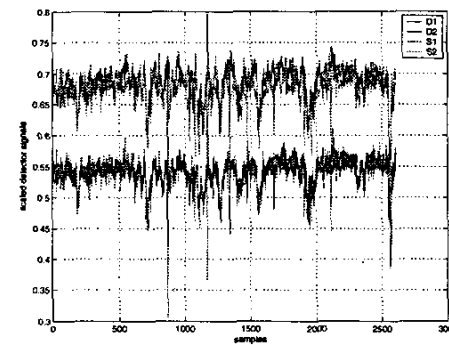


**Figure 6:** Measured detector signals  $D_1(n)$ ,  $D_2(n)$ ,  $S_1(n)$  and  $S_2(n)$  while passing the finger print.

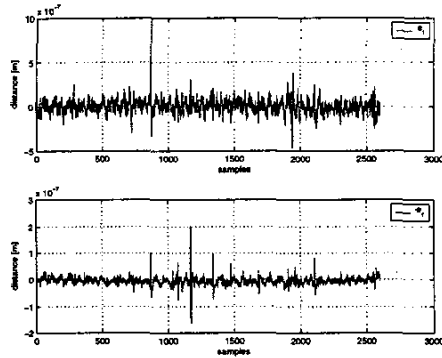


**Figure 7:** Estimated distances  $\hat{e}_f(n)$  and  $\hat{e}_r(n)$  while passing the finger print.

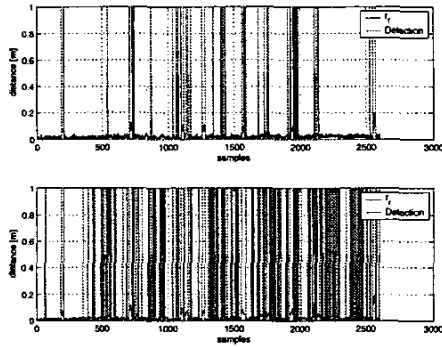


**Figure 8:** The fault parameters  $r_f(n)$  and  $r_r(n)$ , together with their respective fault detections while passing the finger mark.

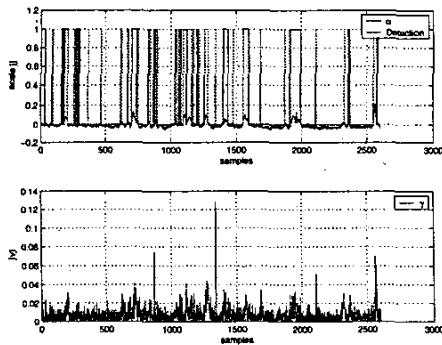


**Figure 9:** The fault parameters  $\alpha(n)$  and  $\gamma(n)$  together with the threshold based fault detection while passing a finger mark.

are a better estimate of the actual focus and radial distances. Notice also the relative large values of  $\hat{e}_f(n)$  and  $\hat{e}_r(n)$  in the start and end of the scratch, these variations are due to heavy controller activates in the start and end of the scratch. From Figs. 4 and 5 it can be seen that  $r_f(n)$ ,  $r_r(n)$  and  $\alpha(n)$  are good fault parameters/ residuals if the purpose is to detect the defect. Based on these residuals a threshold detection is implemented, by using a threshold which give the earliest detection of the scratch without giving false detections. The detections based on the three residuals are for:  $\alpha : n = [236 - 670]$ ,  $r_f : n = [245 - 665]$  and  $r_r : n = [239 - 663]$ . From these it can be seen that  $\alpha(n)$  is more clear for detection than the two others, since the background noise level is lower. An earlier detection of beginning and later detection of the end should be possible. However, using a threshold for detection on one or two of these fault parameters may not be the perfect solution. It can be very useful to apply some kind of time/frequency analysis to the fault parameter(s) to get an even earlier start detection and later end detection. Such an analysis could be based on the discrete wavelet transform. From Fig. 5  $\gamma(n)$  increases while passing the scratch. Meaning that the fault model is not a perfect description of the scratch, but on the other hand not a bad model, since  $\gamma(n)$  inside the scratch is not increased much compared to the outside. It is also seen that increase from the beginning and the decrease at the end of scratch.

The second example is the finger prints, and it seen from the Figs. 6, 8 and 9, that the defect consists of a number of areas where the detector signals are degenerated. This means that the detection can only be on each of these areas, and not between the areas. As for (S) it can be seen that  $r_f(n)$ ,  $r_r(n)$  and  $\alpha(n)$  are good fault parameters, if the parameters are used to detect the fault. By using the threshold detection for this example the detection is switching between being on or off. This is also the physical reality since a finger mark consists of a number of spots on the disc surface and not a large connected defect.  $r_r$  gives more detections, but it is difficult to validate the correctness of these detections.  $\alpha(n)$  gives less detections but they seems more clear due to lower background noise level.

## 6 Conclusion

A Kalman estimator with an internal reference model is designed with the purpose to estimate focus and radial distances,  $\hat{e}_f(n)$  and  $\hat{e}_r(n)$ , in a CD player. These are better as inputs to controllers, controlling the focus and radial loops since these distances decoupled from each other, in contrast to the method used in commercial CD players. The Kalman estimator uses calculated distances as sensor signals, these are found by solving the inverse problem of the optical model of the CD player. Two pairs of two fault parameters are designed, based on  $\hat{e}_f(n)$ ,  $\hat{e}_r(n)$ ,  $\hat{e}_f(n)$  and  $\hat{e}_r(n)$ , with the purpose of faster fault detection. The methods are tested on two set, of experimental data of a scratch and a finger print. These tests indicate that

this preprocessing of the measurement signals can be useful both as inputs to a nominal control of the CD player and for fault detection in the CD player, for use in a fault tolerant control scheme.

## 7 Acknowledgement

The authors acknowledge the Danish Technical Research Council, for support to Peter Fogh Odgaard's Ph.D project, which is a part of a larger research project called WAVES (Wavelets in Audio Visual Electronic Systems), grant no. 56-00-0143.

## References

- Andersen, P, T Pedersen, J Stoustrup and E Vidal (2001). Method for improved reading of digital data disc. International patent, no. WO 02/05271 A1.
- Bouwhuis, W, J Braat, A Huijser, J Pasman, G van Rosmalen and K Schouhamer Immink (1985). *Principles of Optical Disc Systems*. Adam Hilger Ltd.
- Franklin, Gene F., J. David. Powell and Michael Workman (1998). *Digital control of dynamic systems*. third ed.. Addison Wesley.
- Odgaard, P.F, J Stoustrup, P Andersen and H.F Mikkelsen (2003a). Fault detection for compact disc players based on redundant and non-linear sensors. Submitted for publication.
- Odgaard, P.F, J Stoustrup, P Andersen and H.F Mikkelsen (2003b). Modelling of the optical detector system in a compact disc player. In: *Proceedings of the 2003 American Control Conference*. Denver, USA.
- Philips (1994). *Product specification: Digital servo processor DSIC2, TDA1301T*. Philips Semiconductors.
- Stan, Sorin G. (1998). *The CD-ROM drive*. Kluwer Academic Publishers.
- Vidal, E, J Stoustrup, P Andersen, T.S Pedersen and H.F Mikkelsen (2001a). Open and closed loop parametric system identification in compact disk players. In: *ACC2001*. Arlington, Virginia.
- Vidal, E, K.G Hansen, R.S Andersen, K.B. Poulsen, J Stoustrup, P Andersen and T.S Pedersen (2001b). Linear quadratic control with fault detection in compact disk players. In: *Proceedings of the 2001 IEEE International Conference on Control Applications*. Mexico City, Mexico.
- Vidal, E, P Andersen, J Stoustrup and T.S Pedersen (2001c). A study on the surface defects of a compact disk. In: *Proceedings of the 2001 IEEE International Conference on Control Applications*. Mexico City, Mexico.